



**HAL**  
open science

## Tan's Contact for Trapped Lieb-Liniger Bosons at Finite Temperature

Hepeng Yao, David Clément, Anna Minguzzi, Patrizia Vignolo, Laurent Sanchez-Palencia

► **To cite this version:**

Hepeng Yao, David Clément, Anna Minguzzi, Patrizia Vignolo, Laurent Sanchez-Palencia. Tan's Contact for Trapped Lieb-Liniger Bosons at Finite Temperature. 2018. hal-01763698v1

**HAL Id: hal-01763698**

**<https://polytechnique.hal.science/hal-01763698v1>**

Preprint submitted on 11 Apr 2018 (v1), last revised 29 Nov 2018 (v2)

**HAL** is a multi-disciplinary open access archive for the deposit and dissemination of scientific research documents, whether they are published or not. The documents may come from teaching and research institutions in France or abroad, or from public or private research centers.

L'archive ouverte pluridisciplinaire **HAL**, est destinée au dépôt et à la diffusion de documents scientifiques de niveau recherche, publiés ou non, émanant des établissements d'enseignement et de recherche français ou étrangers, des laboratoires publics ou privés.

# Tan's Contact for Trapped Lieb-Liniger Bosons at Finite Temperature

Hepeng Yao,<sup>1</sup> David Clément,<sup>2</sup> Anna Minguzzi,<sup>3</sup> Patrizia Vignolo,<sup>4</sup> and Laurent Sanchez-Palencia<sup>1</sup>

<sup>1</sup>*CPHT, Ecole Polytechnique, CNRS, Université Paris-Saclay, Route de Saclay, 91128 Palaiseau, France*

<sup>2</sup>*Laboratoire Charles Fabry, Institut d'Optique, CNRS, Université Paris-Saclay, 2 avenue Augustin Fresnel, F-91127 Palaiseau cedex, France*

<sup>3</sup>*Univ. Grenoble-Alpes, CNRS, LPMMC, F-38000 Grenoble, France*

<sup>4</sup>*Université Côte d'Azur, CNRS, Institut de Physique de Nice, 1361 route des Lucioles, 06560 Valbonne, France*

(Dated: April 11, 2018)

The universal Tan relations connect a variety of microscopic features of many-body quantum systems with two-body contact interactions to a single quantity, called the contact. The latter has become pivotal in the description of quantum gases. We provide a complete characterization of the Tan contact of the harmonically trapped Lieb-Liniger gas for arbitrary interactions and temperature. Combining thermal Bethe ansatz, local density approximation, and exact quantum Monte Carlo calculations, we show that the contact is a universal function of only two scaling parameters, and determine the scaling function. We find that the temperature-dependence of the contact, or equivalently the interaction-dependence of the entropy, displays a maximum. The presence of this maximum provides an unequivocal signature of the crossover to the fermionized regime and it is accessible in current experiments.

Describing strongly-correlated quantum systems from microscopic models and first principles is a central challenge for modern many-body physics. The derivation of universal relations in systems governed by contact interactions is an example of such an approach [1, 2]. Point-like interactions induce a characteristic singularity of the many-body wavefunction at short inter-particle distance and, correspondingly, algebraically decaying momentum tails,  $n(k) \simeq C/k^4$  [3, 4]. The  $1/k^4$  scaling is universal and holds irrespective of the quantum statistics, dimension, temperature, and interaction strength. Furthermore, the weight  $C$  of the tails, known as the Tan contact, contains a wealth of information about many quantities characterizing the specific state, e.g. the interaction energy, the pair correlation function, the free-energy dependence on interactions, and the relation between pressure and energy density [1, 2, 4]. Stemming from the unique possibility to measure it in cold-atom gases, the contact has become central to the description of quantum gases. Recent experiments on three-dimensional Fermi and Bose gases have permitted to validate the universal Tan relations, hence demonstrating that  $C$  provides valuable information on a variety of thermodynamic quantities [5–10].

Interacting one-dimensional (1D) bosons display very different physical regimes at varying interaction strength, from quasicondensates to the emblematic *fermionization* effect [11]. So far, emergence of statistical transmutation in the Tonks-Girardeau regime [12, 13] and suppression of pair correlations in the crossover towards strong correlations [14, 15] have been reported in cold-atom experiments. However, the experimental characterization of the various quantum degeneracy regimes at finite temperature, identified in Ref. [16], remains challenging. A major difficulty is that most quantities show a smooth monotonic behaviour when crossing over different regimes. Understanding whether the contact can provide an efficient probe is one of the motivations of our work.

In most experimental conditions, the gases are confined in longitudinal harmonic traps and thermal effects cannot be ne-

glected. While the homogeneous 1D gas is exactly solvable by Bethe ansatz, the trapped system is not integrable, therefore requiring approximate or *ab initio* numerical approaches. Previous theoretical studies have investigated the contact for homogeneous bosons at finite temperature [17, 18], trapped bosons at zero temperature [3, 19], and at finite temperature in the Tonks-Girardeau limit [20]. Momentum distributions of strongly-interacting, trapped bosons at finite-temperature were also computed by quantum Monte-Carlo methods [21].

In this work, we provide a complete characterization of the Tan contact of 1D bosons under harmonic confinement for arbitrary interactions, particle number, temperature, and trap frequency, and show that it indeed provides a useful probe of quantum degeneracy regimes. Using a combination of thermal Bethe-ansatz solutions with local-density approximation and exact quantum Monte Carlo calculations, we demonstrate that the contact is a universal function of only two scaling parameters and find the scaling function (see Fig. 1), hence

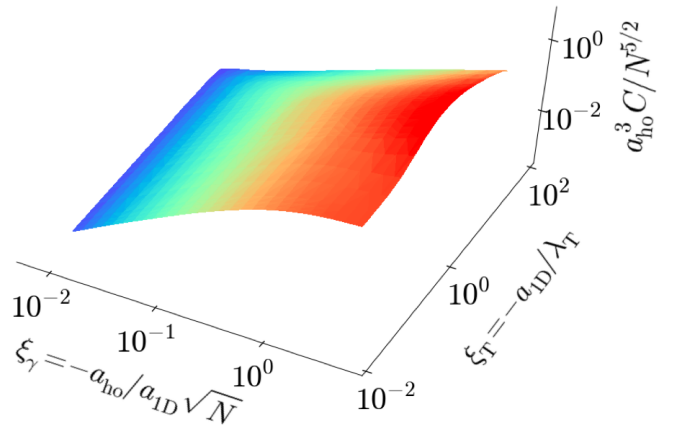


Figure 1. (Color online) Reduced Tan contact  $a_{ho}^3 C / N^{5/2}$  for 1D Bose gases in a harmonic trap, versus the reduced temperature  $\xi_T = -a_{1D} / \lambda_T$  and the reduced interaction strength  $\xi_\gamma = -a_{ho} / a_{1D} \sqrt{N}$ . The results are found using thermal Bethe ansatz solutions combined with local density approximation (see main text).

generalizing the results of Ref. [21]. As a main result, we find that the contact displays a maximum versus the temperature. This behaviour is characteristic of the trapped gas with finite, although possibly arbitrary strong, interactions. We argue that the existence of this maximum is a direct consequence of the dramatic change of correlations and thus provides an unequivocal signature of the crossover to fermionization in the trapped 1D Bose gas. We derive asymptotic limits and discuss a physical picture of the evolution of the contact versus temperature and interaction strength. Finally, we compute the full momentum distributions in various regimes. They show the emergence of the high-momentum tails and assess the experimental observability of our predictions.

*Two-parameter scaling.*— Consider a 1D Bose gas with repulsive two-body contact interactions, in the presence of the harmonic potential  $V(x) = m\omega^2 x^2/2$ , with  $m$  the particle mass,  $x$  the space coordinate, and  $\omega/2\pi$  the trap frequency. It is governed by the extended Lieb-Liniger (LL) Hamiltonian

$$\mathcal{H} = \sum_j \left[ -\frac{\hbar^2}{2m} \frac{\partial^2}{\partial x_j^2} + V(x_j) \right] + g \sum_{j < \ell} \delta(x_j - x_\ell), \quad (1)$$

where  $j$  and  $\ell$  span the set of particles, and  $g = -2\hbar^2/m a_{1D}$  is the coupling constant with  $a_{1D}$  the 1D scattering length. The thermodynamic properties of the interacting gas at the finite temperature  $T$  are uniquely determined by the grand-potential  $\Omega = -k_B T \ln [\text{Tr} e^{-(\mathcal{H} - \mu \mathcal{N})/k_B T}]$ , where  $k_B$  is the Boltzmann constant,  $\mathcal{N}$  the particle number operator, and  $\mu$  the chemical potential.

We start from the homogeneous case,  $V(x) = 0$ . Using  $k_B T$  as the unit energy and, correspondingly, the thermal de Broglie wavelength  $\lambda_T = \sqrt{2\pi\hbar^2/mk_B T}$  as the unit length, we readily find that the Hamiltonian  $\mathcal{H}/k_B T$  is a function of the unique parameter  $a_{1D}/\lambda_T$ . Since the interactions are short range,  $\Omega$  is an extensive quantity. It follows that the dimensionless quantity  $\Omega/k_B T$  is a function of the sole intensive, dimensionless parameters  $\mu/k_B T$  and  $a_{1D}/\lambda_T$ , times the length ratio  $L/\lambda_T$ . We may thus write

$$\Omega/k_B T = (L/\lambda_T) \mathcal{A}_h(\mu/k_B T, a_{1D}/\lambda_T), \quad (2)$$

with  $\mathcal{A}_h$  a dimensionless function.

For the gas under harmonic confinement, the additional energy scale  $\hbar\omega$  emerges, associated to the length scale  $a_{ho} = \sqrt{\hbar/m\omega}$ . Within the local-density approximation (LDA), we write the grand potential as the sum of the contributions of slices of homogeneous LL gases with a chemical potential locally shifted by the trap potential energy,  $\Omega/k_B T = \int \frac{dx}{\lambda_T} \mathcal{A}_h[\mu - V(x), T, g]$ . Using Eq. (2) and rescaling the position  $x$  by the quantity  $2\sqrt{\pi} a_{ho}^2/\lambda_T$ , we then find

$$\Omega/k_B T = (a_{ho}/\lambda_T)^2 \mathcal{A}(\mu/k_B T, a_{1D}/\lambda_T), \quad (3)$$

where  $\mathcal{A}$  a dimensionless function stemming from  $\mathcal{A}_h$ . The scaling forms of the relevant thermodynamics quantities are then readily found from Eq. (3). On the one hand, the average

particle number,  $N = -\partial\Omega/\partial\mu|_{T, a_{1D}}$ , reads

$$N = (a_{ho}/\lambda_T)^2 \mathcal{A}_N(\mu/k_B T, a_{1D}/\lambda_T). \quad (4)$$

It follows that the reduced chemical potential  $\mu/k_B T$  is a universal function of only two scaling parameters, namely  $N\lambda_T^2/a_{ho}^2$  and  $a_{1D}/\lambda_T$ , or, equivalently,  $\xi_\gamma = -a_{ho}/a_{1D}\sqrt{N}$ , and  $\xi_\tau = -a_{1D}/\lambda_T$ . On the other hand, the contact is expressed using the Tan sweep relation [4, 22, 23],  $C = (4m/\hbar^2) \partial\Omega/\partial a_{1D}|_{T, \mu}$ , yielding  $C = (a_{ho}^2/a_{1D}^5) \mathcal{A}_C(\mu/k_B T, a_{1D}/\lambda_T)$ . Using Eq. (4) and writing  $\mu/k_B T$  as a function of  $\xi_\gamma$  and  $\xi_\tau$ , we find

$$C = \frac{N^{5/2}}{a_{ho}^3} f(\xi_\gamma, \xi_\tau), \quad (5)$$

with  $f$  a dimensionless function. In the following, we shall use this two-parameter scaling form. Note that the choice of the scaling parameters is not unique, but any other choice can be related to ours. For instance, the parameters  $2mk_B T/\hbar^2 \rho(0)^2$  and  $mg/\hbar^2 \rho(0)$  identified in Ref. [21] can be related to those in Eq. (5) by noting that the density at the trap center  $\rho(0)$ , multiplied by  $\lambda_T$ , is a function of  $\xi_\tau$  and  $\xi_\gamma$ . Our choice of the parameters is motivated by the fact that they only depend on bulk quantities. Note also that the procedure used to find the scaling form (5) is general and can be straightforwardly extended to higher dimensions and Fermi gases.

*Scaling function for 1D bosons at finite temperature.*— In order to verify the scaling form (5) and find the scaling function  $f$  for interacting 1D bosons, we use two complementary approaches.

On the one hand, we perform the LDA on the exact solutions of the Yang-Yang (YY) equations [24], found by the thermal Bethe ansatz for the grand-potential density

$$\Omega/L = -k_B T \int \frac{dq}{2\pi} \ln \left[ 1 + e^{-\frac{\epsilon(q)}{k_B T}} \right], \quad (6)$$

and the dressed energy,

$$\epsilon(k) = \frac{\hbar^2 k^2}{2m} - \mu - k_B T \int \frac{dq}{2\pi} \frac{2c}{c^2 + (k-q)^2} \ln \left[ 1 + e^{-\frac{\epsilon(q)}{k_B T}} \right], \quad (7)$$

with  $c = mg/\hbar^2 = -2/a_{1D}$ . We thus find the grand potential in the harmonic trap, and the scaling function  $\mathcal{A}$  in Eq. (3). Applying the procedure presented above, we then find the scaling function  $f$  in Eq. (5) for the contact.

On the other hand, to assess the accuracy of the LDA, we perform *ab-initio* quantum Monte Carlo (QMC) calculations. We use the same implementation as in Refs. [25, 26]. The continuous-space path integral formulation allows us to simulate the exact Hamiltonian (1), for an arbitrary trap  $V(x)$ , within the grand-canonical ensemble. The statistical average of the number of world lines yields the total number of particles  $N$ , and the interaction energy  $\langle \mathcal{H}_{\text{int}} \rangle$  is computed from the zero-range two-body correlator. The contact is then found using the thermodynamic relation

$$C = (2gm^2/\hbar^4) \langle \mathcal{H}_{\text{int}} \rangle. \quad (8)$$

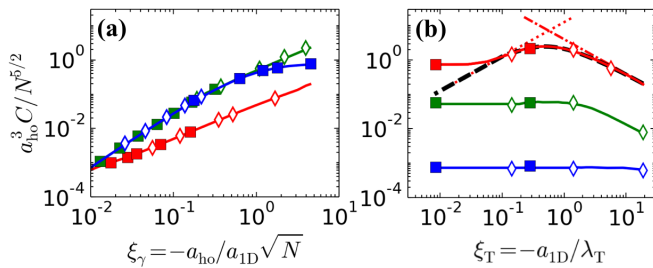


Figure 2. (Color online) Reduced Tan contact  $a_{\text{ho}}^3 C / N^{5/2}$  versus the scaling parameters, as found from LDA (solid lines) and QMC calculations (points). (a) Reduced contact versus the interaction strength  $\xi_\gamma = -a_{\text{ho}}/a_{1\text{D}}\sqrt{N}$  at the fixed temperatures corresponding to  $\xi_T = -a_{1\text{D}}/\lambda_T = 0.0085$  (blue), 0.28 (green), and 18.8 (red). (b) Reduced contact versus the temperature via the quantity  $\xi_T$  at the fixed interaction strengths  $\xi_\gamma = 10^{-2}$  (blue),  $1.58 \times 10^{-1}$  (green), and 4.47 (red). The black dashed, red dotted, and red dash-dotted lines correspond to Eq. (S12), Eq. (10), and Eq. (11) respectively. The QMC data are found from various sets of parameters, corresponding to the various symbols [30].

The world lines are discretized into an adjustable number  $M$  of slices of elementary imaginary propagation time  $\epsilon = 1/Mk_B T$  each, and sampled using the worm algorithm [27, 28]. Each calculation is run for various values of  $\epsilon$  and polynomial extrapolation is used to eliminate systematic finite-time discretization errors [29].

The scaling function  $f$ , namely the rescaled contact  $a_{\text{ho}}^3 C / N^{5/2}$ , for 1D bosons under harmonic confinement resulting from YY theory and LDA is shown in Fig. 1. Figure 2 shows some lettersections of the latter (solid lines) along with QMC data (points) for a quantitative comparison. The rescaled contact is plotted as a function of the interaction strength  $\xi_\gamma$  for various values of the temperature via the quantity  $\xi_T$  in Fig. 2(a) and, inversely, as a function of  $\xi_T$  for various values of  $\xi_\gamma$  in Fig. 2(b). The numerically-exact QMC data are computed for a broad set of parameters. When plotted in the rescaled units of Eq. (5), they show excellent data collapse among each other and fall onto the LDA curves. Quite remarkably, the agreement holds also in the low-temperature and strongly-interacting regime where the particle number is as small as  $N \simeq 5$ , within less than 3%. Our analysis hence validates the scaling form (5) and shows that the LDA is very accurate in computing the contact for the trapped LL model.

*Onset of a maximum contact versus temperature.*— We now turn to the behavior of the contact. Particularly interesting is the non-monotonicity of  $C$  versus the temperature and the onset of a maximum, see Fig. 2(b). This behaviour strongly contrasts with those found for the homogeneous gas and the trapped gas in the Tonks-Girardeau limit ( $a_{1\text{D}} \rightarrow 0$ ), which are both characterized by a systematic increase of the contact versus temperature [17, 20]. In the trapped case, the maximum in the contact as a function of  $\xi_T$  is found irrespective to the strength of interactions but is significantly more pronounced in the strongly-interacting regime. From the data of Fig. 1, we extract the temperature  $T^*$  at which the contact

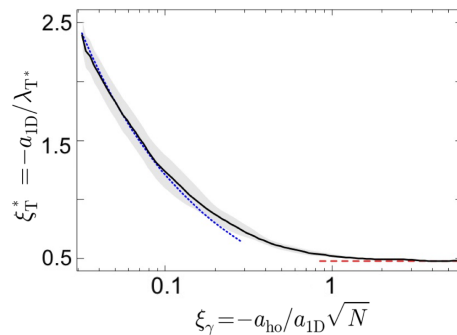


Figure 3. (Color online) Behaviour of the temperature at which the contact is maximum versus the interaction strength. Shown is the value of  $\xi_T^*$  (solid black line) as found from the data of Fig. 1, together with the asymptotic behaviours  $\xi_\gamma^* \simeq 0.49$  for the strongly-interacting regime (dashed red line) and  $\xi_\gamma^* \propto \xi_\gamma^{\nu_{\text{int}}}$ , with  $\nu_{\text{int}} \simeq 0.6$  for the weakly-interacting regime (dotted blue line).

is maximum at fixed  $\xi_\gamma$ . In Fig. 3, we plot  $\xi_T^* = -a_{1\text{D}}/\lambda_T^*$  as a function of  $\xi_\gamma$ . As we discuss now,  $\xi_T^*$  shows significantly different behaviours in the strongly- and weakly-interacting regimes, but, in both cases, it characterizes the onset of the regime dominated by interactions.

We first consider the strongly-interacting regime,  $\rho(0)|a_{1\text{D}}| \lesssim 1$ . Using the virial expansion, we obtain the analytical expression for the contact [29]

$$C = \frac{2N^{5/2}}{\pi a_{\text{ho}}^3} \frac{\xi_\gamma}{\xi_T} \left( \sqrt{2} - \frac{e^{1/2\pi\xi_T^2}}{\xi_T} \text{Erfc}(1/\sqrt{2\pi}\xi_T) \right), \quad (9)$$

see black dashed line in Fig. 2(b). It has a maximum at  $\xi_T^* = 0.485$ , in very good agreement with the asymptotic scaling  $\xi_T^* \simeq 0.490 \pm 0.005$  extracted from the data (dashed red line in Fig. 3).

The existence of a maximum of the contact in the strongly-interacting regime can be inferred by a competition of two different behaviours. On the one hand, at low temperatures,  $|a_{1\text{D}}| \lesssim \lambda_T$  ( $\xi_T \lesssim 1$ ), both quantum and thermal fluctuations are dominated by the repulsive interactions and the gas is fermionized. The contact is then found from the Bose-Fermi mapping, i.e.  $C = (2\hbar^2/gm) \int dx \rho(x)e_\kappa(x)$ , where  $e_\kappa$  is the kinetic-energy density [31]. Since the gas is weakly degenerate, the latter follows from the equipartition theorem, i.e.  $e_\kappa(x) = \rho(x)k_B T/2$ , and the density profile can be taken as non-interacting, i.e.  $\rho(x) = (N/\sqrt{2\pi}L_{\text{th}}) \exp(-x^2/2L_{\text{th}}^2)$ , with  $L_{\text{th}} = \sqrt{k_B T/m\omega^2}$ . It yields

$$C = 2\sqrt{2}N^{5/2}\xi_\gamma\xi_T/a_{\text{ho}}^3, \quad \xi_\gamma^{-1} \lesssim \xi_T \lesssim 1, \quad (10)$$

thus recovering the results of Ref. [20] by a different approach.

On the other hand, at high temperature,  $\lambda_T \lesssim |a_{1\text{D}}|$  ( $\xi_T \gtrsim 1$ ), the weakly-degenerate Bose gas is dominated by thermal fluctuations. In this case, the contact can be estimated by the mean-field expression  $\langle \mathcal{H}_{\text{int}} \rangle = g \int dx \rho(x)^2$ . Using the ther-

mal density profile, we then find

$$C \simeq 2\sqrt{2}N^{5/2}\xi_\gamma/\pi\xi_\tau a_{\text{ho}}^3, \quad \xi_\gamma^{-1}, 1 \lesssim \sqrt{\xi_\tau}. \quad (11)$$

Both Eqs. (10) and (11) are in good agreement with the numerical calculations, see red dotted and dash-dotted lines in Fig. 2(b). These expressions show that the contact increases with the temperature in the fermionized regime but decreases when thermal fluctuations dominate over interactions. The maximum of the contact thus provides a non-ambiguous signature of the crossover to fermionization.

The situation is completely different in the weakly-interacting regime,  $\rho(0)|a_{\text{1D}}| \gtrsim 1$ . In this case, the gas is never fermionized. At low temperature,  $(|a_{\text{1D}}|/\rho(0)^3)^{1/4} \lesssim \lambda_T$ , the gas forms a quasi-condensate characterized by suppressed density fluctuations [17]. The contact is then found from the mean-field expression for  $\langle \mathcal{H}_{\text{int}} \rangle$ , using the Thomas-Fermi (TF) density profile  $\rho(x) = (\mu/g)(1 - x^2/L_{\text{TF}}^2)$  with  $L_{\text{TF}} = \sqrt{2\mu/m\omega^2}$ . In this regime one has [3]

$$C = \eta N^{5/2} \xi_\gamma^{5/3} / a_{\text{ho}}^3, \quad 1, \xi_\tau \lesssim \xi_\gamma^{-1} \quad (12)$$

with  $\eta = 4 \times 3^{2/3}/5$ .

In the high-temperature and weakly-interacting regime,  $\lambda_T \lesssim (|a_{\text{1D}}|/\rho(0)^3)^{1/4}$ , the interactions are negligible and the bosons form a nearly ideal degenerate gas. Using the corresponding density profile  $\rho(x) = \lambda_T^{-1} \text{Li}_{1/2}[\exp(\alpha - x^2/2L_{\text{th}}^2)]$  with  $\alpha(\xi_\gamma, \xi_\tau) = \ln[1 - \exp(-1/(2\pi\xi_\gamma^2\xi_\tau^2))]$ , we find

$$C = \left(16\sqrt{\pi}N^{5/2}\xi_\gamma^5\xi_\tau^3/a_{\text{ho}}^3\right) G(\alpha), \quad \xi_\gamma^{-1} \lesssim \xi_\tau \lesssim \xi_\gamma^{-2} \quad (13)$$

with  $G(\alpha) = \int dx \text{Li}_{1/2}^2[\exp(\alpha - x^2)]$ . The function  $G(\alpha)$  decays at least as  $\lambda_T^4$  and thus  $C$  decreases with the temperature. Therefore, in the weakly-interacting regime, the maximum contact signals the crossover from the quasi-condensate regime to the ideal Bose gas regime. The position of the maximum of the contact may be estimated by equating Eqs. (12) and (13). The calculation is significantly simplified by neglecting quantum degeneracy effects in Eq. (13). Then,  $G(\alpha) \simeq \sqrt{\pi/2} \exp(2\alpha)$  and we find

$$\xi_\tau^* \sim \xi_\gamma^{-\nu}, \quad \nu = 2/3. \quad (14)$$

The numerical data are well fitted by Eq. (14) with  $\nu$  as an adjustable parameter (see dotted blue line in Fig. 3), yielding  $\nu_{\text{fit}} = 0.6 \pm 0.06$ , in good agreement with the theoretical estimate  $\nu_{\text{th}} = 2/3$  [32].

*Maximum entropy versus interaction strength.*— To further interpret the onset of a maximum contact versus temperature, it is fruitful to note that it is equivalent to the onset of a maximum entropy  $S$  versus the interaction strength. For a fixed number of particles, it is a direct consequence of the Maxwell identity [33]

$$\partial C / \partial T|_{a_{\text{1D}}, N} = (4m/\hbar^2) \partial S / \partial a_{\text{1D}}|_{T, N}. \quad (15)$$

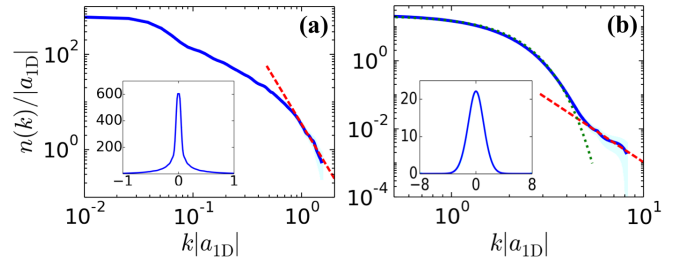


Figure 4. (Colored online) Log-log plots of momentum distributions found by QMC calculations in the strongly-interacting regime. (a) Low temperature:  $\xi_\gamma = 4.47$  and  $\xi_\tau = 0.0085$ . (b) Temperature at the maximum contact:  $\xi_\gamma = 1.26$  and  $\xi_\tau = 0.49$ . The solid blue lines are the QMC results, the dashed red lines are algebraic fits to the large- $k$  tails, and the dotted green lines are the momentum distributions of the non-degenerate ideal gas. The insets show the same data in lin-lin scale.

In the homogeneous LL gas, the entropy at fixed temperature and number of particles, decreases monotonically versus the interaction strength, since the repulsive interactions inhibit the overlap between the particle wavefunctions, hence diminishing the number of available configurations. In the trapped gas, however, this effect competes with the interaction-dependence of the available volume. More precisely, starting from the non-interacting regime, the system size increases sharply with the interaction strength, while the particle overlap varies smoothly. In this regime, the number of available configurations and the entropy thus increase with the interaction strength. At the onset of fermionization, interaction-induced spatial exclusion becomes dramatic and the particles strongly avoid each other. In turn, as opposed to the non-interacting regime, the volume increases very slightly. In this regime, the number of available configurations thus decreases when the interactions increase. This picture confirms that the maximum of the entropy as a function of the interaction strength, or equivalently the maximum of the contact as a function of the temperature, signals the fermionization crossover.

*Experimental observability.*— Our predictions can be checked with ultracold quantum gases where the Tan contact is extracted from radio-frequency spectra or momentum distributions [5, 6, 8, 34]. As an illustration, Fig. 4 shows two examples of momentum distributions as found from QMC calculations in the strongly-interacting regime: Fig. 4(a) corresponds to almost zero temperature ( $\xi_\tau \ll 1$ ) and Fig. 4(b) to the contact maximum ( $\xi_\tau \simeq \xi_\tau^*$ ). In both cases, the momentum distributions exhibit an algebraic decay in the large-momentum tails (note the log-log scale in the main panels), with a weight well agreeing with our estimate for the contact [35]. Note that in the examples shown here the momentum distributions decay over three to four decades. Recent experiments with metastable Helium atoms now cover up to six decades [34] and thus appear particularly suited to extract accurate values of the contact from the diluted large-momentum tails.

*Conclusion.*— Summarizing, we have provided a complete characterization of the Tan contact for the trapped Lieb-Liniger gas with arbitrary interaction strength, number of particles, temperature, and trap frequency. We have derived a universal scaling function of only two parameters and we have shown that it is in excellent agreement with the numerically-exact QMC results over a wide range of parameters. As a pivotal result, we found that the contact exhibits a maximum versus the temperature for any interaction strength. This behaviour is mostly marked in the gas with large interactions and provides an unequivocal signature of the crossover to fermionization. In outlook, the analysis of the Tan contact can be extended to the excited states and multi-component quantum systems. For instance, it can be used to infer the symmetry of the mixtures [36, 37] and of the non-thermal nature of quantum states [38, 39].

P.V. acknowledges Mathias Albert for useful discussions. This research was supported by the European Commission FET-Proactive QUIC (H2020 grant No. 641122). It was performed using HPC resources from GENCI-CCRT/CINES (Grant No. c2017056853). D.C. is a member of the Institut Universitaire de France.

- 
- [1] S. Tan, *Generalized virial theorem and pressure relation for a strongly correlated Fermi gas*, Ann. Phys. (NY) **323**, 2987 (2008).
- [2] S. Tan, *Energetics of a strongly correlated Fermi gas*, Ann. Phys. (NY) **323**, 2952 (2008).
- [3] M. Olshanii and V. Dunjko, *Short-distance correlation properties of the Lieb-Liniger system and momentum distributions of trapped one-dimensional atomic gases*, Phys. Rev. Lett. **91**, 090401 (2003).
- [4] S. Tan, *Large momentum part of fermions with large scattering length*, Ann. Phys. (NY) **323**, 2971 (2008).
- [5] J. T. Stewart, J. P. Gaebler, T. E. Drake, and D. S. Jin, *Verification of universal relations in a strongly interacting Fermi gas*, Phys. Rev. Lett. **104**, 235301 (2010).
- [6] R. J. Wild, P. Makotyn, J. M. Pino, E. A. Cornell, and D. S. Jin, *Measurements of Tan's contact in an atomic Bose-Einstein condensate*, Phys. Rev. Lett. **108**, 145305 (2012).
- [7] Y. Sagi, T. E. Drake, R. Paudel, and D. S. Jin, *Measurement of the homogeneous contact of a unitary Fermi gas*, Phys. Rev. Lett. **109**, 220402 (2012).
- [8] C. Luciuk, S. Trotzky, S. Smale, Z. Yu, S. Zhang, and J. H. Thywissen, *Evidence for universal relations describing a gas with  $p$ -wave interactions*, Nat. Phys. **11**, 1 (2016).
- [9] R. J. Fletcher, R. Lopes, J. Man, N. Navon, R. P. Smith, M. W. Zwierlein, and Z. Hadzibabic, *Two- and three-body contacts in the unitary Bose gas*, Science **355**, 377 (2017).
- [10] S. Laurent, M. Pierce, M. Delehay, T. Yefsah, F. Chevy, and C. Salomon, *Connecting few-body inelastic decay to quantum correlations in a many-body system: A weakly coupled impurity in a resonant Fermi gas*, Phys. Rev. Lett. **118**, 103403 (2017).
- [11] M. Girardeau, *Relationship between systems of impenetrable bosons and fermions in one dimension*, J. Math. Phys. **1**, 516 (1960).
- [12] B. Paredes, A. Widera, V. Murg, O. Mandel, S. Fölling, I. Cirac, G. V. Shlyapnikov, T. W. Hänsch, and I. Bloch, *Tonks-Girardeau gas of ultracold atoms in an optical lattice*, Nature (London) **429**, 277 (2004).
- [13] T. Kinoshita, T. Wenger, and D. S. Weiss, *Observation of a one-dimensional Tonks-Girardeau gas*, Science **305**, 1125 (2004).
- [14] T. Kinoshita, T. Wenger, and D. S. Weiss, *Local pair correlations in one-dimensional Bose gases*, Phys. Rev. Lett. **95**, 190406 (2005).
- [15] T. Jacqmin, J. Armijo, T. Berrada, K. V. Kheruntsyan, and I. Bouchoule, *Sub-Poissonian fluctuations in a 1D Bose gas: From the quantum quasicondensate to the strongly interacting regime*, Phys. Rev. Lett. **106**, 230405 (2011).
- [16] D. S. Petrov, G. V. Shlyapnikov, and J. T. M. Walraven, *Regimes of quantum degeneracy in trapped 1D gases*, Phys. Rev. Lett. **85**, 3745 (2000).
- [17] K. Kheruntsyan, D. Gangardt, P. Drummond, and G. Shlyapnikov, *Pair correlations in a finite-temperature 1D Bose gas*, Phys. Rev. Lett. **91**, 040403 (2003).
- [18] M. Kormos, G. Mussardo, and A. Trombettoni, *Expectation values in the Lieb-Liniger Bose gas*, Phys. Rev. Lett. **103**, 210404 (2009).
- [19] A. Minguzzi, P. Vignolo, and M. Tosi, *High momentum tail in the Tonks gas under harmonic confinement*, J. Phys. Lett. A **294**, 222 (2002).
- [20] P. Vignolo and A. Minguzzi, *Universal contact for a Tonks-Girardeau gas at finite temperature*, Phys. Rev. Lett. **110**, 020403 (2013).
- [21] W. Xu and M. Rigol, *Universal scaling of density and momentum distributions in Lieb-Liniger gases*, Phys. Rev. A **92**, 063623 (2015).
- [22] M. Barth and W. Zwerger, *Tan relations in one dimension*, Ann. Phys. (NY) **326**, 2544 (2011).
- [23] Here, we use the normalization condition of the momentum distribution  $\int \frac{dk}{2\pi} n(k) = N$ .
- [24] C. N. Yang and C. P. Yang, *Thermodynamics of a one-dimensional system of bosons with repulsive  $\delta$ -function interaction*, J. Math. Phys. **10**, 1115 (1969).
- [25] G. Carleo, G. Bo ris, M. Holzmann, and L. Sanchez-Palencia, *Universal superfluid transition and transport properties of two-dimensional dirty bosons*, Phys. Rev. Lett. **111**, 050406 (2013).
- [26] G. Bo ris, L. Gori, M. D. Hoogerland, A. Kumar, E. Lucioni, L. Tanzi, M. Inguscio, T. Giamarchi, C. D'Errico, G. Carleo, et al., *Mott transition for strongly interacting one-dimensional bosons in a shallow periodic potential*, Phys. Rev. A **93**, 011601(R) (2016).
- [27] M. Boninsegni, N. Prokof'ev, and B. Svistunov, *Worm algorithm for continuous-space path integral Monte Carlo simulations*, Phys. Rev. Lett. **96**, 070601 (2006).
- [28] M. Boninsegni, N. V. Prokof'ev, and B. V. Svistunov, *Worm algorithm and diagrammatic Monte Carlo: A new approach to continuous-space path integral Monte Carlo simulations*, Phys. Rev. E **74**, 036701 (2006).
- [29] See Supplemental Material for a detailed description of the finite- $\epsilon$  scaling approach and the derivation of the virial expansion formula.
- [30] For Fig. 2(a), we used  $|a_{1D}|/a_{ho} = 9.5$  (red squares), 0.32 (red diamonds), 1.41 (green squares), 0.14 (green diamonds), 0.14 (blue squares), and 2.02 (blue diamonds). For Fig. 2(b), we used  $|a_{1D}|/a_{ho} = 10$  (blue squares), 31.62 (blue diamonds), 0.45 (green squares), 1.41 (green diamonds), 0.14 (red squares) and 0.07 (red diamonds).
- [31] M. A. Cazalilla, *One-dimensional optical lattices and impenetrable bosons*, Phys. Rev. A **67**, 053606 (2003).
- [32] Quantum degeneracy effects tend to increase the value of  $\nu$  for

small values of  $\xi_\gamma$ . In the asymptotic limit  $\xi_\gamma \rightarrow 0$ , they become dominant and  $G(\alpha) \simeq \pi^2/\sqrt{|\alpha|}$ . We then find the estimate  $\nu = 1$ . However, in this regime, the maximum is extremely weak and hardly visible in practice.

- [33] Equation (15) follows from the sweep relation  $C = (4m/\hbar^2) \partial F/\partial a_{1D}|_{T,N}$  and the thermodynamic definition of the entropy  $S = -\partial F/\partial T|_{a_{1D},N}$ , where  $F(N, T, a_{1D}) = \Omega(\mu, T, a_{1D}) + \mu N$  is the Helmholtz free energy.
- [34] R. Chang, Q. Bouton, H. Cayla, C. Qu, A. Aspect, C. I. Westbrook, and D. Clément, *Momentum-resolved observation of thermal and quantum depletion in a Bose gas*, Phys. Rev. Lett. **117**, 235303 (2016).
- [35] Fitting the tails of the momentum distributions found from the QMC calculations by  $n(k) \simeq C_{\text{fit}}/k^{p_{\text{fit}}}$ , we obtain the following results for  $p_{\text{fit}}$  and  $\tilde{C}_{\text{fit}} = a_{\text{ho}}^3 C_{\text{fit}}/N^{5/2}$ . For Fig. 4(a),  $p_{\text{fit}} = 3.80 \pm 0.20$  and  $\tilde{C}_{\text{fit}} = (1.01 \pm 0.14) \times 10^{-3}$  while  $\tilde{C} \simeq 0.97 \times 10^{-3}$ . For Fig. 4(b),  $p_{\text{fit}} = 3.72 \pm 0.10$  and  $\tilde{C}_{\text{fit}} = 0.23 \pm 0.04$  while  $\tilde{C} \simeq 0.22$ . The agreement with the expected exponent  $p = 4$  is better than 7% and with the contact  $C$  better than 5%.
- [36] J. Decamp, J. Jünemann, M. Albert, M. Rizzi, A. Minguzzi, and P. Vignolo, *High-momentum tails as magnetic-structure probes for strongly correlated  $SU(\kappa)$  fermionic mixtures in one-dimensional traps*, Phys. Rev. A **94**, 053614 (2016).
- [37] J. Decamp, P. Armagnat, B. Fang, M. Albert, A. Minguzzi, and P. Vignolo, *Exact density profiles and symmetry classification for strongly interacting multi-component Fermi gases in tight waveguides*, New J. Phys. **18**, 055011 (2016).
- [38] M. Kormos, Y.-Z. Chou, and A. Imambekov, *Exact three-body local correlations for excited states of the 1D Bose gas*, Phys. Rev. Lett. **107**, 230405 (2011).
- [39] A. Johnson, S. S. Szigeti, M. Schemmer, and I. Bouchoule, *Long-lived nonthermal states realized by atom losses in one-dimensional quasicondensates*, Phys. Rev. A **96**, 013623 (2017).

## Supplemental Material for Tan's Contact for Trapped Lieb-Liniger Bosons at Finite Temperature

In this supplemental material, we provide a detailed description of the finite- $\epsilon$  scaling approach (Sec. S1) and the derivation of the virial-expansion formula (Sec. S2).

### S1. FINITE- $\epsilon$ SCALING IN THE QUANTUM MONTE CARLO CALCULATIONS

The quantum Monte Carlo (QMC) calculations use a continuous-space description of the worm lines within the path-integral formulation. In turn, the imaginary-time (temperature) is discretized with the finite time step  $\epsilon$ . The QMC results are exact in the  $\epsilon \rightarrow 0$  limit. In order to find the final results reported on the Fig. 2 of the main paper, we proceed as follows. For each set of physical parameters (interaction strength, chemical potential, temperature, and trap frequency), we perform a series of QMC calculations for different values of  $\epsilon$  and extrapolate the result to the limit  $\epsilon \rightarrow 0$ .

For most of the calculations, we are able to use a sufficiently small value of  $\epsilon$  and a linear extrapolation is sufficient. We fit the QMC data with  $a_{\text{ho}}^3 C/N^{5/2} = a + b(\epsilon/\beta)$ , with  $a$  and  $b$  as fitting parameters. We then use the quantity  $a$  as the final results of  $a_{\text{ho}}^3 C/N^{5/2}$ . An example is shown on the left panel of Fig. S1 below. In this case, the linear extrapolation only corrects the QMC result for the smallest value of  $\epsilon$  ( $\epsilon/\beta = 0.01$ ) by less than 4%.

In some cases, however, the linear fit is not sufficient for extrapolating correctly the QMC results. This occurs in the strongly-interacting regime for low to intermediate temperatures. In such cases, we use a third-order polynomial,  $a_{\text{ho}}^3 C/N^{5/2} = a + b(\epsilon/\beta) + c(\epsilon/\beta)^2 + d(\epsilon/\beta)^3$ , to extrapolate the finite- $\epsilon$  numerical data. An example is shown on the right panel of Fig. S1. In this case, the extrapolation corrects the QMC result for the smallest value of  $\epsilon$  ( $\epsilon/\beta = 0.0005$ ) by roughly 25%.

For all the QMC results reported on the Fig. 2 of the main paper, we have performed a systematic third-order polynomial extrapolation, even when a linear extrapolation was sufficient.

### S2. DERIVATION OF THE TAN CONTACT IN THE LARGE-TEMPERATURE AND LARGE-INTERACTION LIMIT

We derive here Eq. (9) of the main paper for the contact at large, finite temperature ( $k_B T \gg N\hbar\omega$ ) and large interactions  $|a_{\text{1D}}|/a_{\text{ho}} \ll 1$ . As a first step, the Tan's contact at large temperature and arbitrary interactions can be estimated using the first term of the virial expansion [20]

$$C = \frac{4m\omega}{\hbar\lambda_T} N^2 c_2 \quad (\text{S1})$$

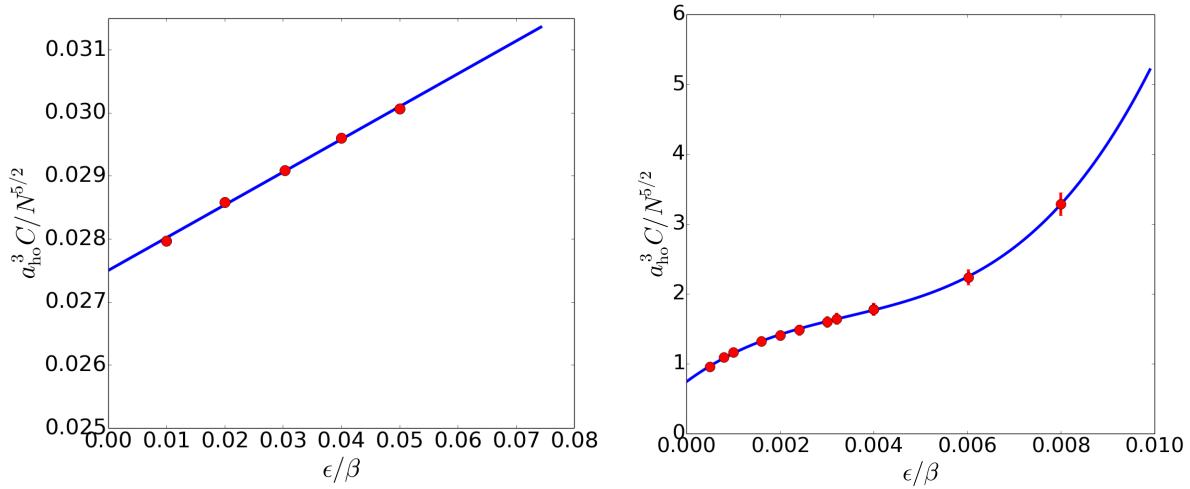


Figure S1. Quantum Monte Carlo (QMC) results for the reduced Tan contact for  $\xi_{\text{T}} = |a_{\text{1D}}|/\lambda_T = 0.28$  and  $\xi_{\text{Y}} = a_{\text{ho}}/|a_{\text{1D}}|\sqrt{N} = 0.1$  (left panel) and for  $\xi_{\text{T}} = 0.0085$  and  $\xi_{\text{Y}} = 4.47$  (right panel). The red points show the QMC results for various values of the dimensionless parameter  $\epsilon/\beta$ , where  $\beta = 1/k_B T$  is the inverse temperature, together with a linear (left panel) or third-order polynomial (right panel) fit.

where  $c_2 = \lambda_T \frac{\partial b_2}{\partial |a_{\text{ID}}|}$  and  $b_2 = \sum_{\nu} e^{-\beta \hbar \omega (\nu + 1/2)}$ . The  $\nu$ 's are the solutions of the transcendental equation

$$f(\nu) = \frac{\Gamma(-\nu/2)}{\Gamma(-\nu/2 + 1/2)} = \sqrt{2} \frac{a_{\text{ID}}}{a_{\text{ho}}}. \quad (\text{S2})$$

By exploiting the Euler reflection formula

$$\Gamma(z)\Gamma(1-z) = \frac{\pi}{\sin(\pi z)}, \quad (\text{S3})$$

one can re-write Eq. (S2) under the form

$$f(\nu) = -\cot(\pi\nu/2) \frac{\Gamma(\nu/2 + 1/2)}{\Gamma(\nu/2 + 1)}. \quad (\text{S4})$$

By using the asymptotic expansions

$$\Gamma(z) \simeq \sqrt{2\pi} z^{z-1/2} e^{-z} \left( 1 + \frac{1}{12z} + O(1/z^2) \right) \quad (\text{S5})$$

and

$$\Gamma(z + 1/2) \simeq \sqrt{2\pi} z^z e^{-z} \left( 1 - \frac{1}{24z} + O(1/z^2) \right), \quad (\text{S6})$$

we obtain the following asymptotic expression for  $f(\nu)$

$$f(\nu) \simeq -\cot(\pi\nu/2) \frac{1}{\sqrt{\nu/2 + 1/2}} \simeq -\sqrt{\frac{2}{\nu}} \cot(\pi\nu/2). \quad (\text{S7})$$

In the Tonks-Girardeau regime, corresponding to  $a_{\text{ID}} = 0$ , one has  $\nu = 2n + 1$ , with  $n \in \mathbb{N}$ . Thus, in the regime  $|a_{\text{ID}}|/a_{\text{ho}} \ll 1$ , we obtain an explicit expression for  $\nu$ , by writing

$$\sqrt{\frac{2}{2n+1}} \cot(\pi\nu/2) \simeq \sqrt{2} \frac{|a_{\text{ID}}|}{a_{\text{ho}}} \quad (\text{S8})$$

namely

$$\nu_n = \frac{2}{\pi} \text{acot}(\sqrt{2n+1} |a_{\text{ID}}|/a_{\text{ho}}) + 2n, \quad n \in \mathbb{N}. \quad (\text{S9})$$

This yields the following explicit expression for  $c_2$ :

$$\begin{aligned} c_2 &= \lambda_T \sum_{\nu} (-\beta \hbar \omega) \frac{\partial \nu}{\partial |a_{\text{ID}}|} e^{-\beta \hbar \omega (\nu_n + 1/2)} \\ &= \lambda_T \sum_n (-\beta \hbar \omega) \frac{2}{\pi} \frac{\sqrt{2n+1}}{a_{\text{ho}}} \frac{-1}{1 + (2n+1) \frac{a_{\text{ID}}^2}{a_{\text{ho}}^2}} e^{-\beta \hbar \omega (\nu_n + 1/2)} \\ &= \frac{2\lambda_T \beta \hbar \omega}{\pi a_{\text{ho}}} \sum_n \frac{\sqrt{2n+1}}{1 + (2n+1) \frac{a_{\text{ID}}^2}{a_{\text{ho}}^2}} e^{-\beta \hbar \omega (\nu_n + 1/2)}. \end{aligned} \quad (\text{S10})$$

In order to evaluate analytically the sum in Eq. (S10), we replace  $\nu$  with  $2n + 1$  in the exponential. Indeed, the first-order correction in  $|a_{\text{ID}}|$  gives a negligible contribution in the limit  $\beta \rightarrow 0$  and  $a_{\text{ID}} \rightarrow 0$ . We finally get

$$c_2 = \sqrt{2} \left( \frac{1}{2\pi \xi_{\text{T}}^2} - \frac{e^{1/2\pi \xi_{\text{T}}^2}}{2^{3/2} \pi \xi_{\text{T}}^3} \text{Erfc}(1/\sqrt{2\pi} \xi_{\text{T}}) \right). \quad (\text{S11})$$

Thus, the contact at large temperatures and large interactions can be approximated by

$$\begin{aligned} C &= \frac{4\sqrt{2}N^2}{|a_{\text{ID}}| a_{\text{ho}}^2 \xi_{\text{T}}} \left( \frac{1}{2\pi \xi_{\text{T}}^2} - \frac{1}{2^{3/2} \pi \xi_{\text{T}}^3} e^{1/2\pi \xi_{\text{T}}^2} \text{Erfc}(1/\sqrt{2\pi} \xi_{\text{T}}) \right) \\ &= \frac{2N^{5/2}}{\pi a_{\text{ho}}^3} \frac{\xi_{\text{T}}}{\xi_{\text{T}}} \left( \sqrt{2} - \frac{e^{1/2\pi \xi_{\text{T}}^2}}{\xi_{\text{T}}} \text{Erfc}(1/\sqrt{2\pi} \xi_{\text{T}}) \right). \end{aligned} \quad (\text{S12})$$

We have verified that this expression is in excellent agreement with the calculation of Eq. (S1) using the numerical solution of Eq. (S2), see Fig. S2.

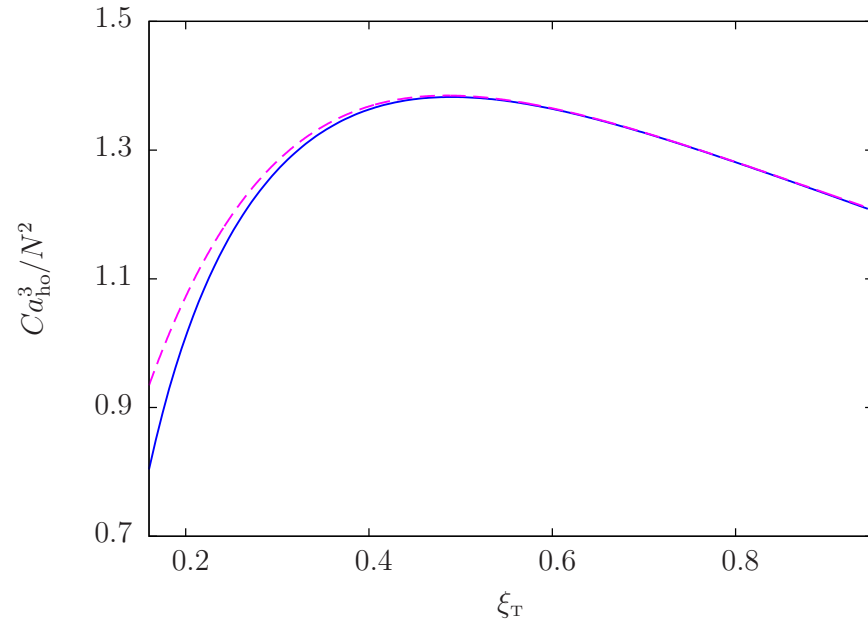


Figure S2.  $Ca_{ho}^3/N^2$  calculated using the numerical solution of Eq. (S2) (blue continuous line) and using the analytical expression (S12) (magenta dashed line). We have considered  $|a_{1D}|/a_{ho} = 0.4$ .